PERGAMON

International Journal of Heat and Mass Transfer 41 (1998) 2857–2864

International Journal of HEAT and MASS TRANSFER

Rotary heat exchanger performance with axial heat dispersion

Sankar Nair, Samir Verma, S. C. Dhingra*

Department of Chemical Engineering, Indian Institute of Technology, Hauz Khas, New Delhi 110016, India

Received 27 October 1995

Abstract

A model of the rotary heat exchanger accounting for axial heat dispersion and longitudinal matrix conduction is developed. The heat conservation equations are solved using a finite difference approach. The heat exchanger effectiveness is then predicted and the effect of axial heat dispersion on the exchanger performance is studied.

Nomenclature

Ag cross-sectional fluid area for dispersion in a zone (with subscript)
Ag^* ratio of Ag_n to Ag_m
As cross-sectional matrix area for conduction in a zone (with subscript)
As^* ratio of As_n to As_m
C thermal capacity rate (with appropriate subscript)
D fluid dispersion coefficient
E_1 effectiveness without dispersion
E_2 effectiveness with dispersion
hA heat transfer coefficient times area for a zone
hA^* ratio of hA_n to hA_m
k matrix thermal conductivity
L matrix length
NTU no. of fluid transfer units (with subscript)
NTU_o no. of overall transfer units
Pe^{-1} overall fluid Peclet number
Pe_m^{-1} overall matrix Peclet number
R matrix radius
t fluid temperature, dimensionless
T matrix temperature, dimensionless
z length coordinate
z^* dimensionless length coordinate, z/L.

Greek symbols

β_n zone n dispersion parameter
δ ratio of D_n to D_m
ε matrix porosity
θ_f fluid temperature
θ_{mt} matrix temperature
θ_1 fluid entry temperature, zone m
θ_2 fluid entry temperature, zone n
λ_n zone n conduction parameter
ϕ angle coordinate
ϕ^* dimensionless angle coordinate, ϕ/ψ
ψ zone angle.

Subscripts

i z-direction
j ϕ-direction
m maximum fluid
M number of z-divisions
n minimum fluid
r matrix
R, S no. of columns in each zone

1. Introduction

Rotary heat exchangers presently find applications as regenerators for steam boilers, vehicle gas-turbine installations, and airconditioning systems. They possess high performance and provide large heat transfer area per unit volume (upwards of 400 m^2 per m^3).

Earlier models of rotary heat exchangers considered only the convection and exchange terms in the energy balances [1, 2, 4], neglecting the effects of longitudinal matrix

* Corresponding author.

0017-9310/98 $19.00
PII: S0017-9310(98)00004-0

conduction and axial dispersion of the fluids. Later investigators included the effects of longitudinal matrix conduction but neglected the effect of axial dispersion on the performance of rotary heat exchangers [3, 7].

The dispersion model is generally used to account for the effects of axial heat conduction, turbulent eddies and vortices on the transport of energy. It is essentially a plug flow model with molecular and macroscopic dispersion of energy superimposed on it. Roetzel and Xuan [8] employed the dispersion model to account for the effect of shell side flow maldistribution on the transient behavior of multipass shell and of tube heat exchangers. Das and Roetzel [9] presented a dynamic analysis of plate heat exchangers based on the dispersion model which takes into consideration the deviation from ideal plug flow in both fluids to predict the response to temperature transients. The purpose of this paper is to develop a model for a counterflow rotary heat exchanger that takes into account the axial dispersion of heat in both fluids in addition to the matrix conduction and exchange terms. The simplifying assumptions made are:

(1) Steady state operation.
(2) Thermal properties of the two fluids and matrix are constant with time and temperature.
(3) The fluids are in counterflow and the matrix rotates on a fixed axis.
(4) The conductivity of the matrix is negligible along the direction of rotation, finite along the fluid flow direction and infinite in the radial direction.
(5) The convective heat transfer coefficients are constant along the length.
(6) Dispersion is finite in the fluid-flow direction, negligible along the direction of rotation and infinite in the radial direction.
(7) The fluids enter at uniform and steady temperatures.
(8) There is no intermixing of the two fluids.

Estimates of the axial thermal dispersion coefficients (D) for packed beds can be obtained from [5] and [6].

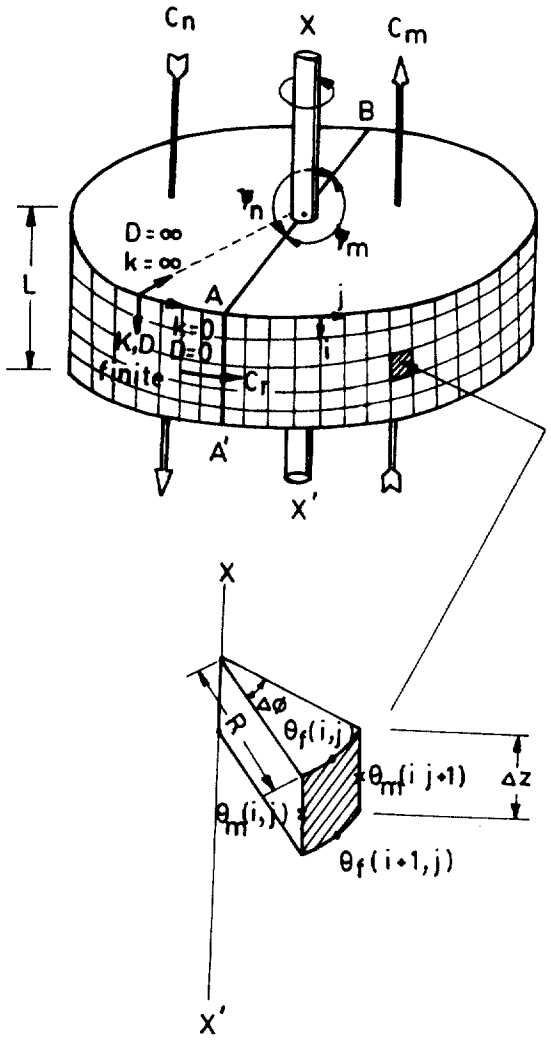

Fig. 1. Representation of the rotary regenerator.

2. Method

Figure 1 represents an axial flow rotary heat exchanger [3]. Since the matrix conductivity is infinite along the radial direction and the fluid perfectly mixed in this direction, there are no radial temperature gradients. The regenerator may therefore be discretized using the grid shown in the figure. If the elements are considered to be fixed in space, each element can be considered as a cross flow heat exchanger with a matrix and a fluid stream. Although the elements are actually three-dimensional triangular slices, a two-dimensional grid corresponding to the shaded area of the element is used since the fluid and matrix temperatures are uniform in the radial direction. Each element is, therefore, bounded by four temperatures, viz. the inlet and outlet fluid and matrix temperatures.

For convenience, the grid is cut along the line AA′ to assume the form shown in Fig. 2. It may be noted that the temperatures on the left and right edges of the grid are physically the same, since they correspond to the same line AA′. Hence $T_m(i, 1) = T_n(M+1-i, s)$. Further, the temperatures shown on the boundary between the two zones are physically the same for each zone. A typical element in each zone is shaded. The fluid with the higher thermal capacity rate (the 'maximum' fluid) enters the regenerator at temperature θ_1 and the 'minimum fluid' enters at temperature θ_2. The temperatures are made dimensionless by the following definitions:

$$\text{Fluid}: t = \frac{(\theta_f - \theta_2)}{(\theta_1 - \theta_2)}$$

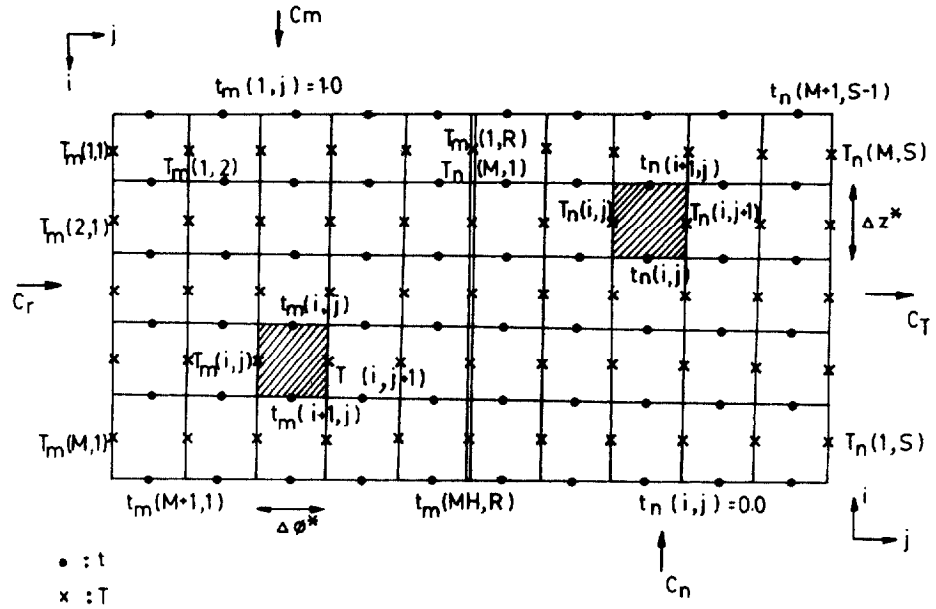

Fig. 2. Coordinate system and schematic representation.

$$Matrix: T=\frac{(\theta_{mt}-\theta_2)}{(\theta_1-\theta_2)}.$$

2.1. Overall energy balance for a typical element on the side of the maximum fluid

Considering the energy balance for an element, the energy transferred to the element by convection, conduction and dispersion equals the energy stored in the element. The energy balance for a typical element on the maximum fluid side (the side of C_m) may be written as:

$$C_m\frac{\Delta\phi_m}{\psi_m}[t_m(i,j)-t_m(i+1,j)] \quad (1)$$

$$+k\left[(1-\varepsilon)\frac{R^2}{2}\Delta\phi_m\right]\times\frac{\left(\frac{T_m(i-1,j)+T_m(i-1,j+1)}{2}-\frac{T_m(i,j)+T_m(i,j+1)}{2}\right)}{\Delta z} \quad (2)$$

$$-k\left[(1-\varepsilon)\frac{R^2}{2}\Delta\phi_m\right]\times\frac{\left(\frac{T_m(i,j)+T_m(i,j+1)}{2}-\frac{T_m(i+1,j)+T_m(i+1,j+1)}{2}\right)}{\Delta z} \quad (3)$$

$$+D\left[\varepsilon\frac{R^2}{2}\Delta\phi_m\right]\left(\frac{t_m(i-1,j)-2t_m(i,j)+t_m(i+1,j)}{2\Delta z}\right) \quad (4)$$

$$-D\left[\varepsilon\frac{R^2}{2}\Delta\phi_m\right]\left(\frac{t_m(i,j)-2t_m(i+1,j)+t_m(i+2,j)}{2\Delta z}\right) \quad (5)$$

$$=C_r\frac{\Delta z}{L}[T_m(i,j+1)-T_m(i,j)]. \quad (6) \quad (1)$$

The terms in equation (1) are

(1) Net energy in by convection
(2) Energy in by matrix conduction. The term in square brackets is the area of the element available for conduction
(3) Energy out by matrix conduction
(4) Energy in by axial heat dispersion
(5) Energy out by axial heat dispersion
(6) Energy stored in the element.

C_m = mass flow rate of fluid × specific heat of fluid.
C_r = mass flow rate of matrix × specific heat of matrix.

2.2. Energy balance on the fluid

For an element on the side of C_m, the rate of heat transfer by convection and dispersion equals the rate of change in enthalpy of the fluid across the element. A second equation is thus obtained:

$$(hA)_m \frac{\Delta\phi_m}{\psi_m}\cdot\frac{\Delta z}{L}(\Delta T)_{avg} + D\left[\varepsilon\frac{R^2}{2}\Delta\phi_m\right]\left(\frac{t_m(i-1,j)-2t_m(i,j)+t_m(i+1,j)}{2\Delta z}\right) - D\left[\varepsilon\frac{R^2}{2}\Delta\phi_m\right]\left(\frac{t_m(i,j)-2t_m(i+1,j)+t_m(i+2,j)}{2\Delta z}\right) = C_m\frac{\Delta\phi_m}{\psi_m}[t_m(i+1,j) - t_m(i,j)] \quad (2)$$

where $(\Delta T)_{avg}$ is the mean temperature difference between the fluid and the matrix in the element. For small element size, this may be taken as the arithmetic mean difference:

$$(\Delta T)_{avg} = \left[\frac{t_m(i,j)+t_m(i+1,j)}{2} - \frac{T_m(i,j)+T_m(i,j+1)}{2}\right].$$

2.3. Boundary conditions

For the maximum fluid, the Danckwerts boundary condition at the entrance of the exchanger is written as

$$C_m\frac{\Delta\phi_m}{\psi_m}[1-t_m(1,j)] = D\frac{\varepsilon R^2}{2}\Delta\phi_m\left[\frac{t_m(1,j)-t_m(2,j)}{\Delta z}\right]. \quad (3)$$

At the exit, there is no dispersive effect. Hence

$$\frac{dt_m}{dz} = 0. \quad (4)$$

Also, there is no matrix conduction at the ends.

Using the above equations one can solve for the matrix outlet temperatures $T_m(i,j+1)$ and the fluid outlet temperatures $t_m(i+1,j)$. The resulting equations can be written with dimensionless coefficients, given in the Appendix. For the top and bottom row elements in Fig. 2 the equations are modified as per the boundary conditions. For the zone of C_m, the following equations are obtained:

Top Row:

$$T_m(1,j+1) = C_1T_m(1,j)+C_2[T_m(2,j)+T_m(2,j+1)] + C_3[t_m(3,j)-t_m(1,j)]+C_4[1-t_m(2,j)] \quad (5a)$$

$$t_m(2,j) = C_6+(C_7+C_8)[1-t_m(1,j)]+C_7t_m(3,j) + C_8[t_m(1,j)+t_m(1,j+1)]. \quad (5b)$$

Using the Danckwerts boundary condition (3) at the entrance, we also have

$$t_m(1,j) = [2A_4t_m(2,j)+A_1]/(2A_4+A_1). \quad (5c)$$

Middle Rows:

$$T_m(i,j+1) = C_9T_m(1,j)+C_{10}[T_m(i-1,j) + T_m(i-1,j+1)+T_m(i+1,j)+T_m(i+1,j+1)] - C_{11}[t_m(i-1,j)+t_m(i+2,j)] + C_{12}t_m(i,j)-C_{13}t_m(i+1,j) \quad (6a)$$

$$t_m(i+1,j) = C_{14}t_m(i,j)+C_{15}[T_m(i,j)+T_m(i,j+1)] + C_{16}[t_m(i-1,j)+t_m(i+2,j)]. \quad (6b)$$

Bottom Row:

$$T_m(M,j+1) = C_1T_m(M,j)+C_2[T_m(M-1,j) + T_m(M-1,j+1)]-C_3t_m(M-1,j) + C_4t_m(M,j)-C_{17}t_m(M+1,j) \quad (7a)$$

$$t_m(M+1,j) = C_{18}t_m(M,j)+C_{15}[T_m(M,j) + T_m(M,j+1)]+C_{16}t_m(M-1,j). \quad (7b)$$

Similar equations can be derived for the zone of C_n. Here the z-coordinate has been reversed, following the direction of fluid flow as shown in Fig. 2.

3. Computational procedure

The finite-difference equations (5)–(7) show that, to solve for the matrix outlet temperatures, the temperatures of later elements should be known. A three-step computational procedure is used.

3.1. Step 1

The solution for the case of no conduction and no dispersion is first obtained as follows. The coefficients C_2, C_3, C_7, C_{10}, C_{11} and C_{16} are set to zero; $t_m(1,j) = 1$ and $t_n(1,j) = 1$. Considering first the zone of C_m, all the unknown terms vanish except for $t_m(i+1,j)$. This is eliminated from equations (5a)–(7a) by using the corresponding equations (5b)–(7b). The modified expressions in the maximum fluid zone for the no conduction, no dispersion case are:

Top Row:

$$T_m(1,j+1) = \frac{(C_1-C_4C_8)}{(1+C_4C_8)}T_m(1,j) + \frac{(C_5-C_4C_6)}{(1+C_4C_8)}t_m(1,j) \quad (8a)$$

$$t_m(2,j) = C_6t_m(1,j)+C_8[T_m(1,j)+T_m(1,j+1)]. \quad (8b)$$

Middle Rows:

$$T_m(i,j+1) = \frac{(C_9-C_{13}C_{15})}{(1+C_{13}C_{15})}T_m(i,j) + \frac{(C_{12}-C_{13}C_{14})}{(1+C_{13}C_{15})}t_m(i,j) \quad (9a)$$

$$t_m(i+1,j) = C_{14}t_m(i,j)+C_{15}[T_m(i,j)+T_m(i,j+1)]. \quad (9b)$$

Bottom Row:

$$T_m(M,j+1) = \frac{(C_1-C_{15}C_{17})}{(1+C_{15}C_{17})}T_m(M,j) + \frac{(C_4-C_{17}C_{18})}{(1+C_{15}C_{17})}t_m(M,j) \quad (10a)$$

$$t_m(M+1,j) = C_{18}t_m(M,j) + C_{15}[T_m(M,j) + T_m(M,j+1)]. \quad (10b)$$

Similar modifications are made for the minimum fluid zone. A matrix temperature distribution is assumed on the left edge (the 1st column of Fig. 2). Equations (8)–(10) are used to work down the column and obtain the fluid and matrix temperatures for the next column. In this way all temperatures in the maximum fluid are calculated. The borderline temperatures of the maximum fluid are then used as starting values for the minimum fluid zone and the process is repeated, working from the bottom of the minimum fluid zone this time, till the right edge is reached. If the temperature distribution assumed on the left edge was correct then the right edge will give the same values, since they are physically the same. If the values do not agree, the right edge values are assumed as the new left edge values and the computation is repeated for the entire grid. A solution is accepted when the percentage average error between the right edge and left edge temperatures reduces to a specified value (0.00001%). Hence the solution for no conduction and no dispersion is obtained which provides an initial estimate of the temperature distributions.

3.2. Step 2

With the estimated temperatures from Step 1, equations (5)–(7) are used to solve for the no-dispersion case, taking matrix conduction into account. This time only the coefficients C_3, C_7, C_{11} and C_{16} are set to zero. However, no further modifications are necessary because estimates of the temperature distribution have already been obtained from Step 1. By iterating on the grid the no-dispersion solution is obtained. At this stage, the no-dispersion effectiveness (E_1) is computed. By definition:

$$E_1 = \frac{\text{temperature difference of minimum fluid}}{\text{maximum possible difference in the exchanger}}.$$

In the dimensionless temperature scales

$$E_1 = \frac{[t_n(M+1,j)]_{avg} - 0}{1.0 - 0} = [t_n(M+1,j)]_{avg}. \quad (11)$$

3.3. Step 3

Having determined the no-dispersion performance from equation (11) and new temperature estimates, equations (5)–(7) are again solved for the dispersion case taking all the coefficients and the boundary condition (3) into account. The temperature $t_m(1,j)$ is first estimated from (3). After the temperature distributions are obtained by iterating on the grid, the effectiveness with dispersion (E_2) is calculated as in (11).

This being a finite-difference method, the results will vary with the number of subdivisions. Hence the number of ϕ and z subdivisions are increased from 12 to 15 and then to 20 at which the variation in the results becomes negligible. The results for the no-dispersion case are essentially in agreement with those obtained by Bahnke and Howard [3]. In Steps 2 and 3, convergence is considerably improved if two passes per column are made before proceeding to the next. This is due to the interdependence of the fluid and matrix temperatures as seen in the equations. Convergence is faster if better estimates for each column are obtained by making two passes per column, since these are used for further calculations.

4. Results and discussion

The dispersive effect is characterized by the percentage change in effectiveness from the no-dispersion case.

$$\text{Percentage change} = \frac{(E_1 - E_2)}{E_1} \times 100 = \frac{\Delta E_{12}}{E_1} \times 100.$$

To present the results and to study the effects of dispersion the following parameters are defined:

$$NTU_o = \text{overall transfer units} = NTU_n\left[\frac{1}{1+(hA)^*}\right]$$

$$Pe_m^{-1} = \text{inverse matrix Peclet number} = \lambda_n\left[1+\frac{1}{(As)^*}\right]$$

where

$$\lambda_n = \frac{kA_{s_n}}{C_nL}.$$

These parameters are also defined in [3]. In addition, the overall Peclet number for the fluid phase is defined as:

$$Pe^{-1} = \frac{D_mAg_m}{C_nL} + \frac{D_nAg_n}{C_nL} = \frac{D_nAg_n}{C_nL}\left[1+\frac{D_m}{D_n}\cdot\frac{Ag_m}{Ag_n}\right]$$

or

$$Pe^{-1} = \beta_n\left[1+\frac{1}{\delta(Ag)^*}\right].$$

The effectiveness of the heat exchanger obtained from the model is plotted as a function of NTU_o with Pe_m^{-1} as a parameter, for two values of Pe^{-1} (Figs. 3–4). A sample of the results is presented in Table 1 which corresponds to Fig. 4. The effect of dispersion is also presented by plotting the percentage change in effectiveness versus NTU_o with Pe^{-1} as a parameter, for two values of Pe_m^{-1} (Figs. 5–6). Other parameters are kept at the values indicated in the legend. The results of the model for the no-dispersion case (computed using $Pe^{-1} = 0.001$ which causes a negligible dispersion effect) are found to agree (Fig. 4) with the no-dispersion results of Bahnke and Howard [3].

A number of effects are observed from the simulation results:

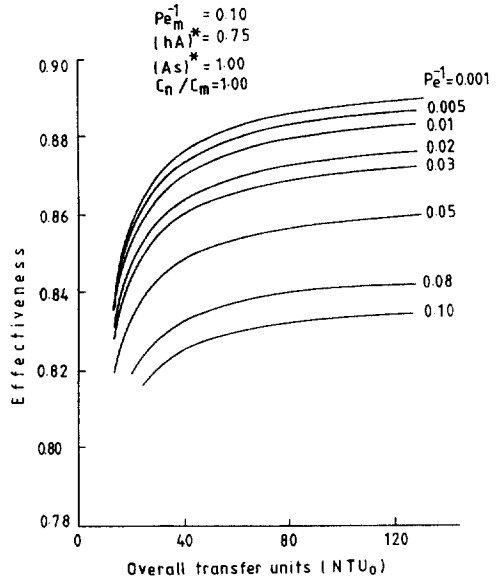

Fig. 3. Effect of heat dispersion on effectiveness.

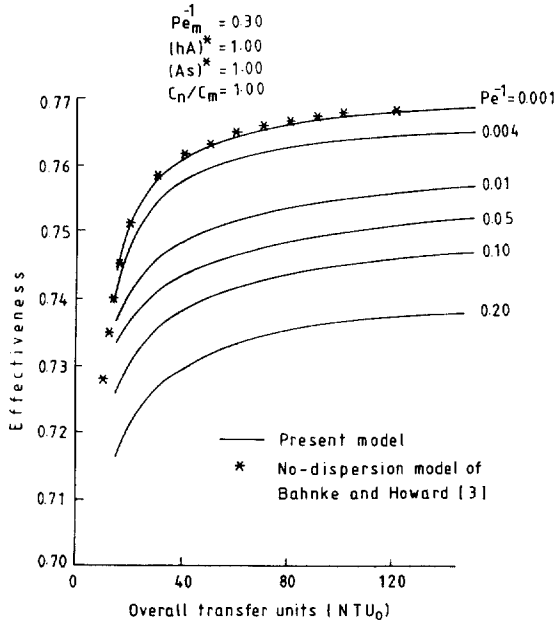

Fig. 4. Effect of heat dispersion on effectiveness.

(1) The effectiveness decreases upon introducing dispersion into the model. This is as expected, due to the axial dispersive heat transfer in the fluid.
(2) Dispersion effects become more significant with rising Pe^{-1} and NTU_o.
(3) Percentage change in effectiveness exhibits two kinds of behavior depending on the magnitudes of the matrix and fluid Peclet numbers. For small values of the matrix number inverse (Pe_m^{-1}), it may pass through a maximum on increasing the overall transfer units (NTU_o), as shown in Fig. 5 where $Pe_m^{-1} = 0.01$. Since in this case the conduction effect is less pronounced, the effectiveness would be close to unity at high NTU_o even accounting for dispersion. Therefore the dispersive effect would cause a lower percentage change in the effectiveness. As the conduction effect becomes more pronounced (for example, Fig. 6 where $Pe_m^{-1} = 0.15$) the percentage change in effectiveness increases asymptotically to a value depending upon the values of the matrix and fluid Peclet numbers.
(4) From the manner in which the parameters are defined, it is expected that the effects of small changes in parameters like δ, $(As)^*$, $(Ag)^*$ and $(hA)^*$ are

Table 1.

	Effectiveness (E_2) Pe^{-1}					
NTU_o	0.001	0.004	0.010	0.050	0.100	0.200
15	0.7411	0.7445	0.7367	0.7334	0.7260	0.7163
20	0.7477	0.7510	0.7409	0.7368	0.7303	0.7210
25	0.7517	0.7550	0.7437	0.7392	0.7332	0.7241
30	0.7544	0.7577	0.7457	0.7410	0.7354	0.7264
35	0.7563	0.7596	0.7473	0.7424	0.7370	0.7282
40	0.7578	0.7611	0.7485	0.7436	0.7384	0.7296
45	0.7589	0.7622	0.7496	0.7445	0.7395	0.7307
50	0.7598	0.7631	0.7505	0.7454	0.7404	0.7317
55	0.7605	0.7639	0.7512	0.7461	0.7412	0.7325
60	0.7611	0.7645	0.7518	0.7467	0.7418	0.7332
65	0.7617	0.7651	0.7524	0.7473	0.7424	0.7338
70	0.7621	0.7655	0.7529	0.7478	0.7430	0.7344
75	0.7625	0.7659	0.7534	0.7482	0.7433	0.7349
80	0.7628	0.7663	0.7538	0.7486	0.7439	0.7354
85	0.7631	0.7666	0.7541	0.7490	0.7442	0.7358
90	0.7634	0.7669	0.7545	0.7494	0.7446	0.7362
95	0.7636	0.7672	0.7548	0.7497	0.7449	0.7366
100	0.7638	0.7674	0.7551	0.7500	0.7452	0.7369
105	0.7640	0.7676	0.7553	0.7502	0.7455	0.7372
110	0.7642	0.7678	0.7556	0.7505	0.7457	0.7375
115	0.7643	0.7680	0.7558	0.7507	0.7459	0.7377
120	0.7645	0.7681	0.7560	0.7510	0.7461	0.7379
125	0.7647	0.7683	0.7562	0.7512	0.7463	0.7381
130	0.7648	0.7684	0.7564	0.7514	0.7465	0.7382
135	0.7649	0.7685	0.7565	0.7515	0.7467	0.7383
140	0.7650	0.7687	0.7567	0.7517	0.7468	0.7384
145	0.7651	0.7688	0.7569	0.7519	0.7470	0.7384
150	0.7652	0.7689	0.7570	0.7520	0.7471	0.7385

$Pe_m^{-1} = 0.30$
$(hA)^* = 1.00$
$(As)^* = 1.00$
$(Ag)^* = 1.00$
$C_n/C_m = 1.00$

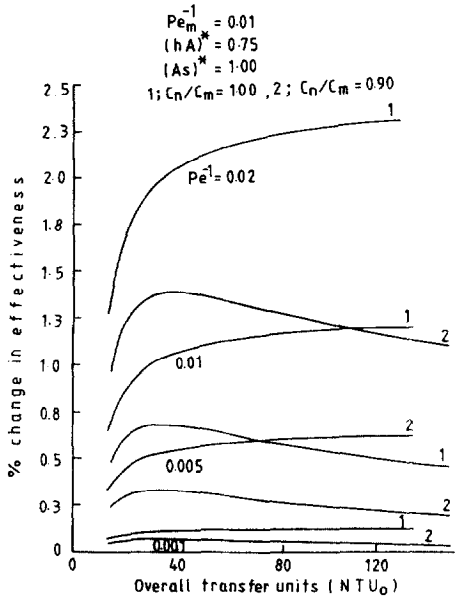

Fig. 5. Effect of Pe^{-1} on percentage change in effectiveness.

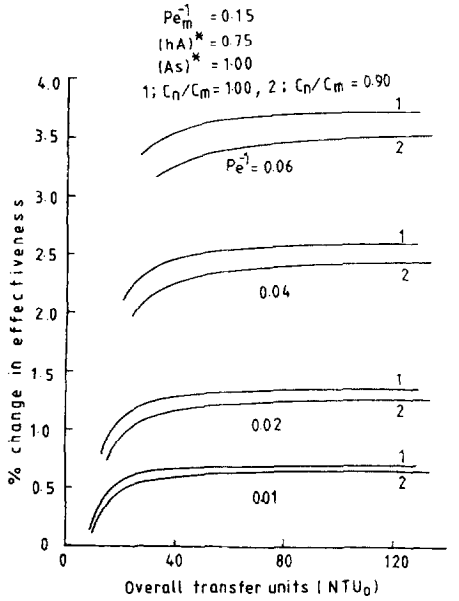

Fig. 6. Effect of Pe^{-1} on percentage change in effectiveness.

negligible. For example, when the simulation is carried out with $Pe_m^{-1} = 0.30$, $\beta_n = 0.05$ and $\delta = 1$, a 25% change in $(Ag)^*$ from 1 to 0.75 changes the value of Pe^{-1} only by 17% (using the definition of Pe^{-1}). This in turn is found to cause only a 0.4% variation in effectiveness at $NTU_o = 20$, and only a 0.5% variation at $NTU_o = 75$. Similar parameter sensitivity results are also reported for the non-dispersive case in [3]. This enables the presentation of the results in a compact form, and the numerical data have therefore been generated for typical values given in the Figure legends.

5. Conclusions

A general numerical method for simulating steady-state counterflow rotary heat exchangers accounting for matrix conduction and fluid dispersion has been developed. Results have been generated over the ranges:

$C_n/C_m = 1.0$ and 0.9

$C_r/C_n = 2.0$

$1 < NTU_o < 120$

$(hA)^* = 0.75$

$(As)^* = 1.0$

$(Ag)^* = 1.0$

$\delta = 1.00$

$0.01 \leqslant Pe_m^{-1} \leqslant 0.30$

$0.001 \leqslant Pe^{-1} \leqslant 0.2.$

The method, however, is not restricted in range. The model shows significant effects of dispersion, especially at higher NTU_o values.

Appendix: Dimensionless coefficients

Define

$$A_1 = \Delta\phi_m^*\Delta z \qquad B_1 = \Delta\phi_n^*\Delta z$$

$$A_2 = \frac{C_r}{C_m}(\Delta z)^2 \qquad B_2 = \frac{C_r}{C_n}(\Delta z)^2$$

$$A_3 = \Delta\phi_m^*\lambda_m/2 \qquad B_3 = \Delta\phi_n^*\lambda_n/2$$

$$A_4 = \Delta\phi_m^*\beta_m/2 \qquad B_4 = \Delta\phi_n^*\beta_n/2$$

$$A_5 = NTU_m\cdot\Delta z/2 \qquad B_5 = NTU_n\cdot\Delta z/2$$

$$A_6 = \frac{\beta_m}{2\Delta z} \qquad B_6 = \frac{\beta_n}{2\Delta z}.$$

Then the coefficients in equations (4)–(6) are:

$$C_1 = \frac{(A_2 - A_3)}{(A_2 + A_3)} \qquad C_{10} = \frac{A_3}{(A_2 + 2A_3)}$$

$$C_2 = \frac{A_3}{(A_2 + A_3)} \qquad C_{11} = \frac{A_4}{(A_2 + 2A_3)}$$

$$C_3 = \frac{A_4}{(A_2 + A_3)} \qquad C_{12} = \frac{(A_1 - A_4)}{(A_2 + 2A_3)}$$

$$C_4 = \frac{A_1}{(A_2 + A_3)} \qquad C_{13} = \frac{(A_1 - A_4)}{(A_2 + 2A_3)}$$

$$C_5 = \frac{(A_1 - A_4)}{(A_2 + A_3)} \qquad C_{14} = \frac{(1 - A_5 - A_6)}{(1 + A_5 + A_6)}$$

$$C_6 = \frac{(1-A_5-A_6)}{(1+A_5)} \qquad C_{15} = \frac{A_5}{(1+A_5+A_6)}$$

$$C_7 = \frac{A_6}{(1+A_5)} \qquad C_{16} = \frac{A_6}{(1+A_5+A_6)}$$

$$C_8 = \frac{A_5}{(1+A_5)} \qquad C_{17} = \frac{(A_1+A_4)}{(A_2+A_3)}$$

$$C_9 = \frac{(A_2-2A_3)}{(A_2+2A_3)} \qquad C_{18} = \frac{(1+A_5)}{(1+A_5+A_6)}.$$

The coefficients for the zone of C_n are similarly obtained, replacing A by B.

References

[1] Lambertson TJ. Performance factors of a periodic-flow heat exchanger. Transactions of ASME 1958;80:586–2.

[2] Mondt JR. Vehicular gas-turbine periodic-flow heat-exchanger solid and fluid temperature distributions. Transactions of ASME J Engg Power 1964;86:121–6.

[3] Bahnke GD, Howard CP. The effect of longitudinal heat conduction on periodic-flow heat exchanger performance. Transactions of ASMEJ Engg Power 1964;86:105–20.

[4] Kays WM, London AL. Compact Heat Exchangers, 2nd edn. McGraw-Hill, 1964.

[5] Gunn DJ, De Souza JFC. Chem Eng Sci 1974;29:1363.

[6] Wakao N. Chem Eng Sci 1976;31:1115.

[7] Skiepko T. Effect of matrix longitudinal heat conduction on temperature fields in the rotary heat exchanger. International Journal of Heat and Mass Transfer 1988;31:2227–38.

[8] Roetzel W, Xuan Y. Analysis of transient behaviour of multipass shell and tube heat exchangers with the dispersion model. International Journal of Heat and Mass Transfer 1992;35:2953–62.

[9] Das SK, Roetzel W. Dynamic analysis of plate heat exchangers with dispersion in both fluids. International Journal of Heat and Mass Transfer 1995;38:1127–40.